

Research



Cite this article: Fodrie FJ, Rodriguez AB, Gittman RK, Grabowski JH, Lindquist NL, Peterson CH, Piehler MF, Ridge JT. 2017 Oyster reefs as carbon sources and sinks. *Proc. R. Soc. B* **284**: 20170891.

<http://dx.doi.org/10.1098/rspb.2017.0891>

Received: 27 April 2017

Accepted: 22 June 2017

Subject Category:

Global change and conservation

Subject Areas:

environmental science, ecology

Keywords:

blue carbon, climate change, ecosystem services, habitat loss, landscape, shellfish

Author for correspondence:

F. Joel Fodrie

e-mail: jfodrie@unc.edu

Electronic supplementary material is available online at <https://dx.doi.org/10.6084/m9.figshare.c.3825517.v4>.

Oyster reefs as carbon sources and sinks

F. Joel Fodrie¹, Antonio B. Rodriguez¹, Rachel K. Gittman², Jonathan H. Grabowski², Niels. L. Lindquist¹, Charles H. Peterson¹, Michael F. Piehler¹ and Justin T. Ridge¹

¹Institute of Marine Sciences, University of North Carolina at Chapel Hill, 3431 Arendell Street, Morehead City, NC 28557, USA

²Marine Science Center, Northeastern University, 430 Nahant Road, Nahant, MA 01908, USA

id FJF, 0000-0001-8253-9648; ABR, 0000-0002-8007-1292; RKG, 0000-0001-8376-8960; MFP, 0000-0003-3881-4862; JTR, 0000-0001-9744-4588

Carbon burial is increasingly valued as a service provided by threatened vegetated coastal habitats. Similarly, shellfish reefs contain significant pools of carbon and are globally endangered, yet considerable uncertainty remains regarding shellfish reefs' role as sources (+) or sinks (−) of atmospheric CO₂. While CO₂ release is a by-product of carbonate shell production (then burial), shellfish also facilitate atmospheric-CO₂ drawdown via filtration and rapid biodeposition of carbon-fixing primary producers. We provide a framework to account for the dual burial of inorganic and organic carbon, and demonstrate that decade-old experimental reefs on intertidal sandflats were net sources of CO₂ ($7.1 \pm 1.2 \text{ MgC ha}^{-1} \text{ yr}^{-1}$ ($\mu \pm \text{s.e.}$)) resulting from predominantly carbonate deposition, whereas shallow subtidal reefs ($-1.0 \pm 0.4 \text{ MgC ha}^{-1} \text{ yr}^{-1}$) and saltmarsh-fringing reefs ($-1.3 \pm 0.4 \text{ MgC ha}^{-1} \text{ yr}^{-1}$) were dominated by organic-carbon-rich sediments and functioned as net carbon sinks (on par with vegetated coastal habitats). These landscape-level differences reflect gradients in shellfish growth, survivorship and shell bioerosion. Notably, down-core carbon concentrations in 100- to 4000-year-old reefs mirrored experimental-reef data, suggesting our results are relevant over centennial to millennial scales, although we note that these natural reefs appeared to function as slight carbon sources ($0.5 \pm 0.3 \text{ MgC ha}^{-1} \text{ yr}^{-1}$). Globally, the historical mining of the top metre of shellfish reefs may have reintroduced more than 400 000 000 Mg of organic carbon into estuaries. Importantly, reef formation and destruction do not have reciprocal, counterbalancing impacts on atmospheric CO₂ since excavated organic material may be remineralized while shell may experience continued preservation through reburial. Thus, protection of existing reefs could be considered as one component of climate mitigation programmes focused on the coastal zone.

1. Introduction

Carbon sequestration is a crucial service provided by marine ecosystems in buffering global climate change. In particular, vegetated coastal habitats, such as salt marshes [1], seagrasses [2] and mangroves [3], are strongly autotrophic ecosystems that fix CO₂ in excess of what is respired and therefore act as disproportionately valuable carbon sinks [4]. This excess carbon is buried in sediments at a rate accounting for roughly 50% of the approximately 250 Tg C buried throughout the entire ocean each year [1]. This burial rate is remarkable considering that these vegetated habitats cover less than 0.5% of seafloor bottom, and troubling given the severe threats facing coastal ecosystems dominated by these foundation species [5]. A dual injury occurs when these habitats are lost, resulting from both the decreased burial capacity of coastal ecosystems, and the release of formerly dormant carbon pools back into the biosphere [3]. As such, there is now national and international momentum to catalogue and protect coastal marine carbon stocks [6,7].

Like vegetated 'blue carbon' habitats, shellfish reefs are severely endangered worldwide (65–85% losses over the last 100 years) [8,9], resulting in forfeiture of several ecosystem services of recognized importance, such as water filtration, denitrification, shoreline stabilization and nursery provision [10]. Moreover, shellfish reefs are uniquely coupled to marine (e.g. phytoplankton, benthic microalgae) and terrestrial (e.g. plant detritus) primary producers via the filtration and subsequent deposition of particulate organic matter (hereafter 'seston') as faeces and pseudofaeces into an accreting reef matrix [11,12]. Without this tight benthic–pelagic coupling and rapid burial mediated by shellfish reefs, seston would remain available for consumption by other heterotrophs that contribute little to carbon burial. Here, we define burial as material that is deposited below the taphonomically active zone (TAZ) of a reef. Therefore, this buried material does not interact with overlying waters or the atmosphere and is potentially stored over centennial to millennial scales [13]. While respiration is a significant carbon transformation within shellfish reefs, the same is true for vegetated coastal habitats that support rich faunal assemblages [14]. Like salt marshes, seagrasses, and mangroves, coupled seston–shellfish reef ecosystems contribute to localized mass burial of newly fixed, excess, organic carbon, and thus may play a notable role in mitigating atmospheric build-up of CO₂.

Recently, carbon burial has been proposed as an incentive for shellfish-reef conservation primarily due to the carbon in shell material [15]. Indeed, carbon sequestration via this pathway is a logical assumption because shellfish build carbonate shells and this material is abundant in the fossil record [13]. However, biosynthesis of calcium carbonate liberates protons from bicarbonate ($\text{Ca}^{2+} + \text{HCO}_3^- = \text{CaCO}_3 + \text{H}^+$), and subsequently contributes to the formation of excess carbonic acid ($\text{H}^+ + \text{HCO}_3^- \rightleftharpoons \text{H}_2\text{CO}_3$) followed by venting of carbon dioxide into the atmosphere ($\text{H}_2\text{CO}_{3\text{aq}} \rightleftharpoons \text{H}_2\text{O} + \text{CO}_2$) [16–18]. Burying this shell has no further direct impacts on atmospheric CO₂, but probably precludes the erosion and dissolution of shell material that would return CO₂ concentrations to pre-shell-formation (i.e. lower) levels. Still, the climate-related consequences of shell production and burial (CO₂ source) and organic carbon deposition (CO₂ sink) within shellfish reefs on carbon cycling are largely additive (but opposite in direction). Thus, the role of shellfish reefs as CO₂ sources or sinks ultimately depends on the relative balance between organic (org-C) and inorganic (inorg-C) carbon burial. Analogous biogeochemical processes occur throughout pelagic ecosystems, where the ratio of diatom (org-C heavy) to coccolithophore (inorg-C heavy) production determines the strength of the regional atmospheric–oceanic CO₂ flux [19,20].

To determine whether shellfish reefs represent CO₂ sources or sinks, quantitative data on burial rates and pools of org-C and inorg-C within this biogenic habitat are needed. Despite a vast literature on shellfish biology and related functions (e.g. alkalinity regulation) [21], few studies have examined emergent shellfish reef properties such as carbon composition and accretion rates (electronic supplementary material, figure S1). Those touting shell burial as a carbon sink have not accounted for the carbonate chemistry that vents CO₂ to the atmosphere during shell biosynthesis, while those excluding oyster reefs as blue-carbon-related habitats may not have included credit for the

rapid burial of recently fixed organic carbon within the reef matrix. In response to these uncertainties, we generated estimates of buried org-C and inorg-C within experimental and natural eastern oyster reefs (*Crassostrea virginica*). Subsequently, we also produced a preliminary, first-order estimate for the CO₂-related outcome of global shellfish habitat loss (oyster reefs, dense aggregations of mussels, etc.) resulting from destructive fishing practices, degraded water quality and shoreline development.

2. Methods

(a) Carbon composition of oyster reefs

We quantified pools and rates of org-C and inorg-C burial within eastern oyster reefs (*C. virginica*) by sampling 19 constructed, experimental reefs and three natural reefs within or near the Rachel Carson National Estuarine Research Reserve (North Carolina; electronic supplementary material, figure S2). The 19 experimental reefs we sampled in the Rachel Carson Reserve were created in 1997 or 2000 (electronic supplementary material, table S1), and are representative of natural reef sizes in this region [22]. These reefs were constructed as $5 \times 3 \times 0.15$ m mounds of 'cultch' shell (electronic supplementary material, figure S3), and developed following natural patterns of oyster recruitment, growth and mortality [23]. Experimental reefs crossed landscapes and inundation regimes, located either on intertidal sandflats ($n = 7$), shallow subtidal sandflats ($n = 3$) or fringing the seaward edge of saltmarsh ($n = 9$), which expanded the generality of our results. To evaluate the representativeness of our experimental-reef data, we also cored one natural intertidal sandflat oyster reef and one natural saltmarsh-fringing oyster reef, as well as one 2.5 m thick relic oyster reef with its top buried 1 m below the sediment surface in the upper North River Estuary (approx. 8 km north of our experimental reefs in the Rachel Carson Reserve). Natural reefs were selected based on their proximity and rough morphological similarity to experimental reefs, and because companion studies provided information on the age of those specific natural reefs necessary for considering the capacity of reefs to support long-term carbon burial. Specifically, an articulated oyster from the base of each natural/relic reef facies was radiocarbon dated at Woods Hole Oceanographic Institution's mass spectrometry facility, and used to estimate the age of these three natural reefs at 45–263 cal yr BP, 0–245 cal yr BP and 4436–4147 cal yr BP, for the intertidal sandflat, saltmarsh-fringing and relic subtidal oyster reefs, respectively. Ages were calibrated to years before present (AD 1950 = 0 BP) at the 95% confidence interval using the CALIB 7.1 program [24].

During 2011, we sampled experimental and natural reefs using a combination of biological (quadrat counts for live oyster density on reefs constructed in 1997; $n = 10$; electronic supplementary material, table S1) and geological (vertical through-reef cores followed by shell and sediment analyses; all reefs; figures 1 and 2; electronic supplementary material, figure S4) methods, as well as three-dimensional laser scanning of experimental reefs to measure reef accretion. To quantify the carbon composition of reefs, we drove 10 cm diameter aluminium pipe vertically through the X–Y centre of each oyster reef using a gas-powered jack hammer. Cores sampled the entire reef structure (10–55 cm deep) and a few decimetres of the underlying substrate. Cores were sectioned continuously in 5 cm vertical increments. To control for carbon burial in the absence of oyster reefs, we examined the carbon composition of sediments beneath experimental reef/cultch material in each core, thus establishing a before–after comparison design. Within each core section, large shell material (more than 2 mm) was separated, washed to remove sediments or shell hash, dried, photographed (electronic supplementary material, figure S5)

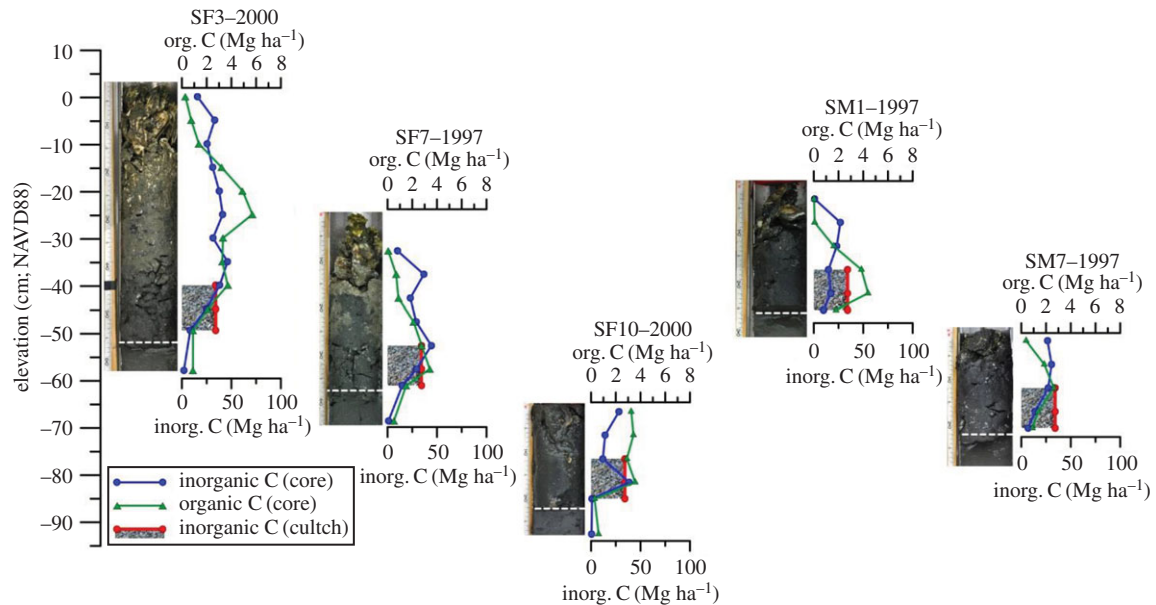


Figure 1. Carbon composition of restored sandflat and saltmarsh-fringing oyster reefs. Org-C (green points/lines) and inorg-C (blue points/lines) data were generated for each 5 cm core section via CHN analyses of sediments and shell weight measurements (with conversions to carbon weights). Five representative reefs are displayed (see electronic supplementary material, figure S4 for complete dataset). For each core photo–profile pair, the white-dashed line represents the base of the experimental reef. The hatched box (bounded in red data points/line) represents the inorg-C used in reef construction in the lowest 15 cm of each reef. Carbon data in cores were generally characterized by mid-reef maxima, reflecting the complex interstices within the taphonomically active zone, as well as dissolution (inorg-C) and lack of biofiltration (org-C) within the cultch shell near the bottom of the reefs, or below in the sandflat unit. Data within each core were vertically integrated to determine carbon burial rates over the lifetime of the reef. Core data are plotted with respect to their absolute vertical position (NAVD88). In labelling each core profile, ‘SF’ designated reefs constructed on sandflats, and the ‘SM’ designated reefs constructed adjacent to saltmarsh. The number immediately following the SF or SM designation identified the replicate number of each reef, and the last four digits note the year in which experimental reefs were established. (Online version in colour.)

and weighed. The remaining sediments and finer-grain shell hash were dried and weighed, and percentage CaCO_3 was determined using an HCl acid digestion. The combined weights of large shells and shell hash were converted to carbon weight based on shell being composed of approximately 11.1% inorganic carbon and less than 0.5% organic carbon [25]. Changes in inorganic carbon weights within reefs between construction (oyster shell cultch) and coring (new growth + cultch) were calculated by subtracting initial (1997 or 2000) from observed (2011) shell weights within each core section (electronic supplementary material, figure S5).

Remaining sediments were dried, ground, fumed with 1N HCl, and re-dried prior to induction in a Perkin Elmer CHN analyzer (Model 2400) to determine percentage organic carbon. Bulk-weight and percentage-carbon data of sediments were combined to quantify org-C in each core section. Measurements of org-C and inorg-C were vertically integrated to produce estimates of carbon in reefs. Before combining org-C and inorg-C data to determine whether reefs functioned as sources or sinks, the influence of total alkalinity on CO_2 partial pressures was accounted for by assuming 0.6 mol of CO_2 release for every 1 mol of carbon bound in shell [16]. These data, combined with explicit knowledge of the age of each reef, allowed determination of annual carbon burial rates.

With these data, we calculated the amount of inorganic carbon within each reef that would have contributed to the venting of CO_2 as: weight of shell (final – cultch weights) \times 0.95 (fraction of inorganic material in shell [25]) \times 0.111 (fraction of carbon, by weight, in CaCO_3 [25]) \times 0.6 (to account for alkalinity of DIC in the ocean). Similarly, we calculated the amount of organic carbon within each reef that would have contributed to the removal of CO_2 as: weight of shell (final – cultch weights) \times 0.0136 (fraction of organic material in shell [25]) \times 0.36 (fraction of carbon, by weight, in organic material [25]) $+$ Σ {weight of sediments in each core section \times approximately 0.0134 (fraction of carbon in sediment, evaluated on a core-section-by-core-

section basis)}. We then subtracted the organic carbon pool from the inorganic carbon pool to determine if reefs were sources (+) or sinks (–). Data were scaled to annual carbon burial/release rates based on the age of each reef on a per hectare basis.

To quantify vertical accretion rates of experimental reefs, digital elevation models (DEMs) of reefs and the surrounding seafloor (used to estimate vertical positions of reef bases; North American Vertical Datum of 1988; hereafter NAVD88) were created using a Riegl LMS-Z210ii terrestrial laser scanner (electronic supplementary material, figure S6). The Riegl system provided three-dimensional resolution of less than 1.5 cm that could be exploited to determine vertical accretion rates (m yr^{-1}) using an endpoint method (i.e. $[\text{height}^{2011} - \text{height}^{\text{initial}}]/[\text{time}]$). Additionally, oyster densities were determined for the experimental reefs constructed in 1997 by collecting multiple, randomly placed 0.25 m^2 quadrat samples on reefs and enumerating all living oysters within each quadrat.

We used a series of regression and ANOVA analyses to explore the patterns and controls of carbon burial in oyster reefs. Regressions compared rates of org-C and inorg-C burial against one another, as well as in relation to reef-scale live-oyster density, vertical position of reefs relative to NAVD88, and reef accretion. Separate regression analyses were run for sandflat (intertidal + subtidal) and saltmarsh-fringing oyster reefs. In all regressions, we used a variant of the Akaike information criterion (AIC) to determine the model order that provided the best fit for the data (balancing model specificity and generality) where: $\text{AIC} = 2k + n[\ln(\text{RSS}/n)]$, and k is the model order, n is the number of observations, and RSS is the residual sum of squares between the observed and fitted data. In all instances except for trends in org-C, inorg-C burial, and CO_2 -relevant carbon flux versus 2010 live oyster densities, a linear fit between variables was determined to be best. In all cases that employed linear fits, we tested whether the slope of data was significantly different from zero. We used ANOVA to consider the CO_2 -related flux of carbon among reefs distributed across various landscape settings and aerial exposures. Data

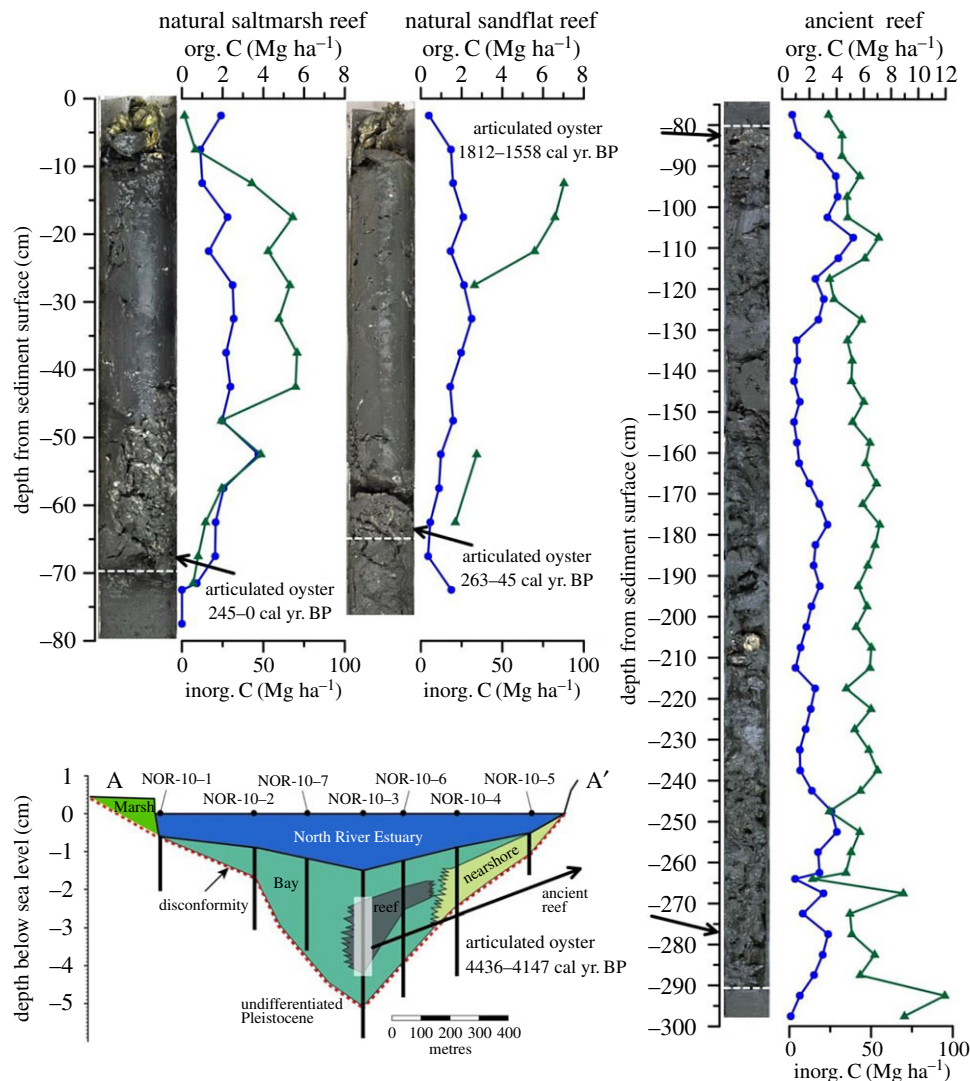


Figure 2. Carbon composition of natural saltmarsh-fringing, sandflat and subtidal relic oyster reefs. Org-C (green points/lines) and inorg-C (blue points/lines) data were generated for each 5 cm core section via CHN analyses of sediments and shell weight measurements (with conversions to carbon weights). For each core photo-profile pair, the white-dashed line represents the lower and upper (ancient reef) limits of reefs. Inset shows where the relic reef core was taken in the North River Estuary (A and A' are included in electronic supplementary material, figure S2, which also shows the location of the two natural reefs). NOR-10-# labels across the inset identify the across-estuary location of additional cores collected to evaluate the distribution of reef material in the system. (Online version in colour.)

from all 19 experimental reefs were included in this ANOVA, with reefs grouped as intertidal sandflat, subtidal sandflat or intertidal saltmarsh-fringing oyster reefs. Data passed F -tests for homoscedasticity ($\alpha = 0.01$). Because a statistically significant difference in CO_2 flux was detected among reefs ($\alpha = 0.05$), we employed Fisher's *post hoc* test (insensitive to unequal sample sizes) to determine which specific group means differed.

(b) CO_2 -related effects of reef disturbance

We combined our data on the inorg-C and org-C stored in the top metre of natural oyster reefs with estimates of historical and extant shellfish reef cover to generate a first-order projection of changes in carbon buried in shellfish habitats following anthropogenic disturbance. While quantitative, site-specific data to constrain the global distribution of shellfish reefs (historic and present) are patchy, there are reliable estimates that estuarine environments cover 125 000 000 ha globally [26] and that within these coastal ecosystems, the cover of shellfish habitat has declined by 65–85% [8,9]. We extracted the data on estuary-by-estuary oyster cover (acreage) in these published shellfish-loss reports, and collected complementary data on the overall size of those same coastal systems to project that shellfish habitat cover within estuaries has declined from 5.1% to 1.9%, on

average, presuming oyster loss rates are in line with other shellfish species. Based on the global footprint of estuaries, this corresponds to a loss of nearly 4 000 000 ha of shellfish habitat (i.e. reefs and aggregations). We combined this estimate with the mean org-C and inorg-C composition (i.e. carbon concentrations: g org-C m^{-3} and g inorg-C m^{-3}) of the three natural and relic reefs we cored to project the amount of carbon disturbed by removing the top 1 m of shellfish habitat from these lost reefs (excluding the TAZ), as well as the carbon pools remaining in the top metre of approximately 2 375 000 ha of extant shellfish habitat (again, excluding the TAZ). We estimated carbon pools/losses in the top metre of reefs to make our results directly comparable to estimates in other blue carbon habitats [2], but acknowledge that in many areas, such as Chesapeake Bay, USA, several metres of reef material could have been removed due to historical fishing or mining [9].

3. Results

(a) Carbon composition of oyster reefs

We found that decade-old oyster reefs had captured $0.3\text{--}2.7 \text{ Mg org-C ha}^{-1} \text{ yr}^{-1}$ (figure 3a), which are burial rates

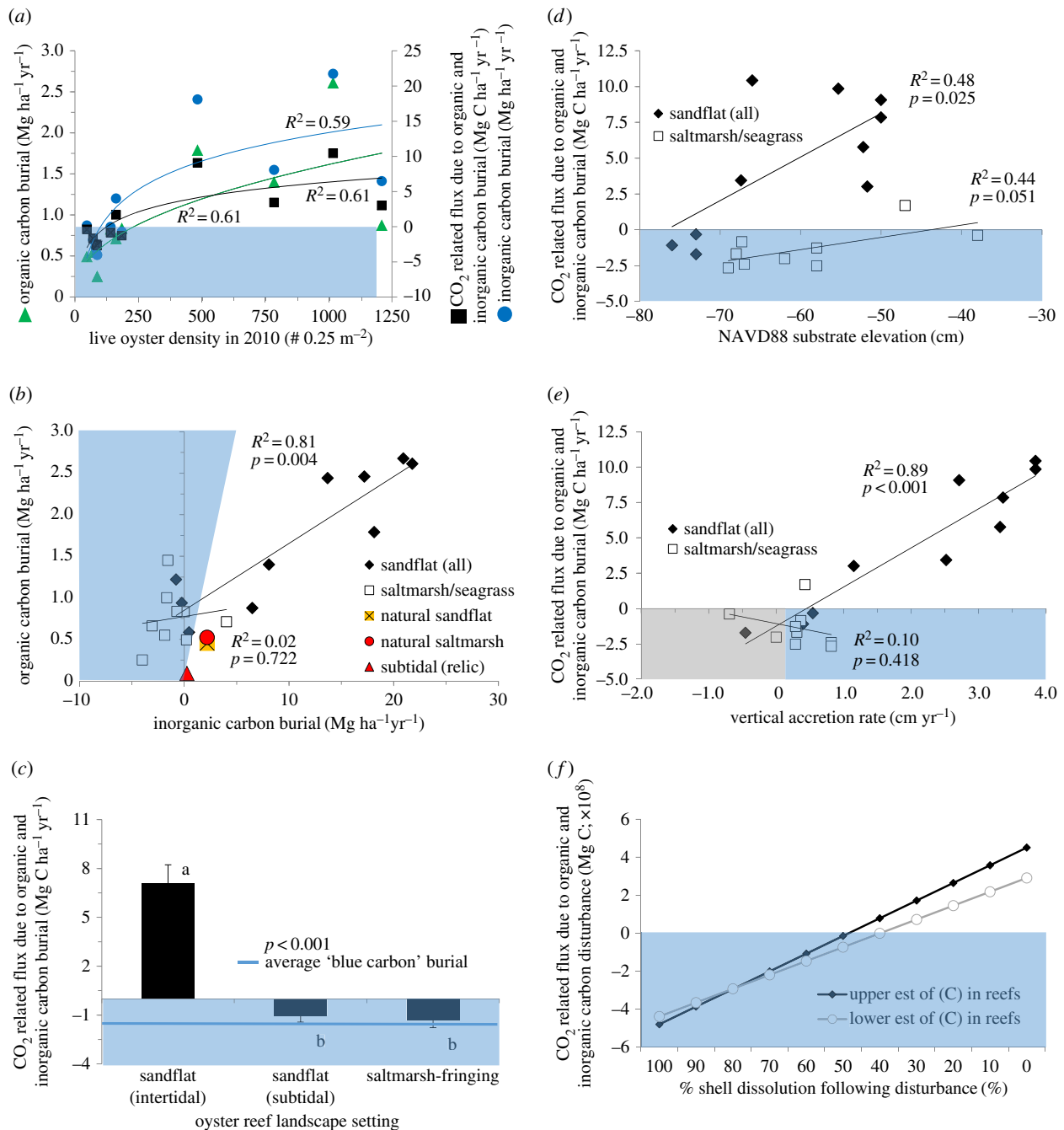


Figure 3. Effects of landscape setting, inundation regime and vertical accretion on org-C burial and inorg-C burial, and together, the climate-related carbon flux into or out of experimental oyster reefs. (a) Org-C and inorg-C burial rates scaled curvilinearly with live oyster density (density data were available for 10 of the 19 reefs included in this study). Following published estimates of 0.6 mol CO₂ production for every mol of CaCO₃ formation (accounting for total alkalinity effects), reefs that functioned as net carbon sinks fall within the blue-shaded region, typically at less than 200 live oysters 0.25 m⁻². (b) Org-C and inorg-C burial were significantly, positively related to each other among sandflat oyster reefs, but not among saltmarsh-fringing oyster reefs. (c) Significant differences were observed in CO₂-related carbon release or burial among intertidal sandflat (95% CI: 1.0–13.1 Mg C ha⁻¹ yr⁻¹) and subtidal sandflat (95% CI: –2.4–0.3 Mg C ha⁻¹ yr⁻¹) or saltmarsh-fringing (95% CI: –4.1–1.4 Mg C ha⁻¹ yr⁻¹) oyster reefs (plotted as $\mu \pm 1$ s.e.), reflecting differences in live oyster densities. Among sandflat oyster reefs, the magnitude and direction of CO₂-related carbon flux was significantly affected by (d) the vertical position of the seafloor on which reefs were constructed and (e) vertical accretion rate, with thresholds apparent at –70 cm NAVD88 and approximately 1.0 cm yr⁻¹, respectively. For saltmarsh-fringing oyster reefs, those factors were not significant. Reefs that functioned as net carbon sinks fall within the blue- or grey-shaded regions (grey: accretion rates of reefs less than sea-level rise, and therefore these reefs are not likely to persist over decadal-centennial scales in the lower portions of estuaries [27]). (f) Net effect of shellfish reef disturbance on atmospheric CO₂ depends primarily on the fate of excavated shell material. Reef disturbance would contribute to CO₂ drawdown if more than 50% of excavated shell material were dissolved. (Online version in colour.)

equivalent to acknowledged blue carbon sinks (global mean: 1.23 Mg org-C ha⁻¹ yr⁻¹) [4,28]. Notably, org-C was almost completely absent in the cored sediments directly beneath reefs which served as our pre-reef controls (figure 1), indicating that reef presence was essential for long-term carbon burial in these sandy environments. Across all reefs, both

org-C and inorg-C burial were related to live oyster density (via filtration, baffling and shell production) (figure 3a). Among sandflat reefs (intertidal + subtidal), org-C and inorg-C burial rates scaled together among ($R^2 = 0.81$; $p = 0.004$; figure 3b) and within ($R^2 = 0.35$; $p < 0.001$; figure 1; electronic supplementary material, figure S4) reefs, although

this pattern was driven mainly by values observed within intertidal reefs (figure 3b). By weight, inorg-C (86% of total carbon) was approximately six times more abundant in intertidal sandflat reefs than org-C (14%). In contrast, org-C burial (68% of total carbon) was approximately double that of inorg-C (32%) within saltmarsh-fringing and subtidal oyster reefs, and there were weak relationships between org-C and inorg-C burial rates among reefs ($R^2 \leq 0.08$; $p \gg 0.05$; figure 3b; electronic supplementary material, figure S4). For subtidal sandflat (three out of three) and saltmarsh-fringing reefs (eight out of nine), coring revealed a net decrease in inorg-C weights as dissolution of cultch material slightly out-paced shell production and burial (initial: $102.8 \text{ Mg inorg-C ha}^{-1}$; figure 3b).

The role of oyster reefs as CO_2 sources or sinks was significantly (ANOVA: $p < 0.001$) affected by landscape setting (Fisher's *post hoc* test comparing intertidal sandflat and intertidal saltmarsh-fringing oyster reefs: $p < 0.001$) and inundation period (Fisher's *post hoc* test comparing intertidal sandflat and subtidal sandflat oyster reefs: $p < 0.001$). Using core data and literature-derived relationships between CaCO_3 formation (1 mol) and CO_2 production (0.6 mol) [16], we determined that intertidal sandflat oyster reefs were net sources of CO_2 ($7.1 \pm 1.2 \text{ Mg C ha}^{-1} \text{ yr}^{-1}$), while subtidal sandflat reefs ($-1.0 \pm 0.4 \text{ Mg C ha}^{-1} \text{ yr}^{-1}$) and saltmarsh-fringing oyster reefs ($-1.3 \pm 0.4 \text{ Mg C ha}^{-1} \text{ yr}^{-1}$) were net carbon sinks (figure 3c). Subtidal sandflat and saltmarsh-fringing oyster reefs that functioned as carbon sinks were characterized by veneers of live oysters (111 ± 19 oysters 0.25-m^{-2}) that contributed to the deposition of organic material without achieving long-term biosynthesis/burial of shell (figure 3c,d). Conversely, intertidal sandflat reefs experience lower levels of predation and bioerosion [27] and were characterized by tightly cemented clusters of live oysters (874 ± 159 individuals 0.25-m^{-2}), resulting in preservation of shell material in the accreting reef matrix (figure 3a–d).

In vegetated estuarine habitats, vertical accretion rates (typically $\leq 1 \text{ mm yr}^{-1}$) scale positively with their carbon burial function [29], but this does not appear to be true for oyster reefs which are among the most rapidly accreting marine biogenic habitats [30]. Our laser scans (electronic supplementary material, figure S6) produced some of the first bioherm-scale measures of vertical accretion by oysters over decadal time scales, showing that the reefs that accreted most rapidly (maximum: 3.85 cm yr^{-1}) were also the largest CO_2 sources (figure 3e). In those reefs, shell material was the main constituent by weight of the accreting matrix (electronic supplementary material, figure S5). While all reefs we identified as CO_2 sources could accrete vertically more quickly than current sea-level rise ($0.25\text{--}0.30 \text{ cm yr}^{-1}$), only 8 of 11 (73%) reefs functioning as carbon sinks appear capable of maintaining their position relative to rising sea levels based on projections for the century ahead (figure 3e).

Carbon pools and burial rates in natural reefs corroborated patterns documented in the decade-old experimental reefs we sampled. Notably, both org-C and inorg-C were present throughout cores of these natural reefs, dating back approximately 250 (intertidal sandflat and saltmarsh fringing) to approximately 4000 years (subtidal, relic) based on radiocarbon dating, confirming that long-term carbon storage is a property of shellfish reefs (figure 2). Down-core profiles of inorg-C within natural reefs (approx. 25 Mg C ha^{-1} in

each 5 cm core section) closely matched patterns from experimental reefs located on intertidal sandflats, but were approximately double the values recorded from experimental saltmarsh-fringing or subtidal reefs (figures 1 and 2). Regardless of landscape, org-C within natural reefs ranged between 2 and 6 Mg C ha^{-1} across depths, on a par with experimental reefs that typically reached values of 4 Mg C ha^{-1} (figures 1 and 2). Overall, org-C accounted for 21% of the carbon stock in natural reefs, and based on their respective ages (figure 2), all three natural reefs functioned as slight CO_2 sources across their entire lifetime ($0.06\text{--}0.83 \text{ Mg C ha}^{-1} \text{ yr}^{-1}$; figure 3b).

(b) CO_2 -related effects of reef disturbance

Estuarine ecosystems span $125\,000\,000 \text{ ha}$ of Earth's surface [26]. While shellfish formerly covered 5.1% of estuarine bottoms, this figure has declined to 1.9% following global habitat loss and degradation (a $3\,989\,000 \text{ ha}$ reduction) [9]. Excluding the TAZ, we estimate that removing the top metre of four million ha of shellfish habitats mobilized $3.71 \times 10^8 \text{ Mg org-C}$ (95% confidence intervals (CI): $2.91\text{--}4.51 \times 10^8 \text{ Mg C}$) and $1.39 \times 10^9 \text{ Mg inorg-C}$ (95% CI: $1.22\text{--}1.55 \times 10^9 \text{ Mg C}$). Presuming that disturbed org-C is remineralized [2], the net effect of shellfish reef disturbance on atmospheric CO_2 depends primarily on the fate of excavated shell material. Were all excavated shell material to be dissolved in seawater, reef disturbance would actually contribute to CO_2 drawdown via the shifting of dissolved inorganic carbon pools away from carbonic acid and towards bicarbonate/carbonate ($-4.61 \times 10^8 \text{ Mg C}$, or $-16.88 \times 10^8 \text{ Mg CO}_2$ scrubbed from the atmosphere) (figure 3f). This is, however, a highly unlikely scenario [21,25]. Rather, excavated shell was probably either reburied in surrounding sediments or extracted and deposited terrestrially. Presuming 100% preservation of excavated shell, global reef disturbance may have led to upwards of $16.88 \times 10^8 \text{ Mg CO}_2$ introduced into the atmosphere ($4.51 \times 10^8 \text{ Mg C}$ respired; figure 3f). We project that $2.2 \times 10^8 \text{ Mg org-C}$ (95% confidence intervals: $1.72\text{--}2.68 \times 10^8 \text{ Mg C}$) and $8.25 \times 10^8 \text{ Mg inorg-C}$ (95% CI: $7.27\text{--}9.23 \times 10^8 \text{ Mg C}$) remain in the top 1 m of extant shellfish reefs.

4. Discussion

In the century ahead, a major challenge for scientists will be to mechanistically describe the controls and consequences of rising greenhouse gas emissions. Like vegetated blue carbon sinks, oyster reefs can be persistent features of estuarine landscapes over millennial time scales, and thus provide a potential repository for long-term organic carbon storage. Major research efforts have characterized carbon pools and fluxes among coastal environments to support inclusion of blue carbon habitats in existing frameworks to combat climate change, such as Nationally Appropriate Mitigation Actions (<http://unfccc.int/focus/mitigation/items/7172.php>). However, no existing international climate mitigation initiatives, such as the Blue Carbon Initiative (<http://thebluecarboninitiative.org>), consider the role of shellfish reefs in burying carbon and enhancing carbon storage in adjacent habitats, nor are there standardized and agreed-upon methodologies for assessing how shellfish reefs influence carbon cycling [28].

Here, we provide an estimate of carbon stocks in Atlantic-coast oyster reefs, and have also developed sound and repeatable methodologies for assessing the net source–sink dynamics of shellfish reefs. This builds from initial work that explored the role of oyster reefs in processing org-C and inorg-C [17,18], and provides entirely new data on the rates and pools of carbon buried within these biogenic habitats. Our results reveal that a subset of restored reefs have functioned as net CO₂ sinks (i.e. saltmarsh fringing and shallow subtidal), which is particularly important in a restoration context for site selection to optimize reef services. Indeed, our data highlight the need to consider landscape context in the siting of future restoration projects to maximize the CO₂-scrubbing services of shellfish reefs. Conversely, our data highlight that CO₂-related climate mitigation is not a service that should be expected/promoted for intertidal reefs constructed over unstructured sandflats.

The carbon storage benefits of conserving or restoring intertidal shellfish reefs may extend beyond the footprint of the reefs themselves. Remarkably, nearly half of all the fringing-saltmarsh reefs constructed in the Rachel Carson Reserve have facilitated localized, seaward expansion of saltmarsh, a recognized blue carbon habitat (figure 4). This indirect blue carbon function of shellfish reefs, not observed at paired control sites (i.e. saltmarsh edges without constructed reefs monitored since 1997) [23], probably occurred because oyster reefs serve as natural breakwaters, dampening wave energy and increasing sediment deposition and stabilization. Ultimately, this appears to have led to the accretion of the surrounding seafloor to a depth suitable for saltmarsh plant (*Spartina alterniflora*) recruitment and growth [29,31]. Thus, the overall blue-carbon-related services of marsh-fringing oyster reefs are potentially conservative given that we did not account for reef-mediated expansion (i.e. facilitation) of this adjacent habitat that also promotes the rapid burial of carbon. This dynamic could be considered in efforts to restore coastal systems using a landscape-level approach, in which the synergies of functions among multiple, interacting habitats are acknowledged.

While carbon stocks in natural reefs provide confidence that our experimental reefs are valuable models, we acknowledge some important nuances that merit further investigation. For instance, all three natural reefs functioned as carbon sources as they accreted. While this should be expected for the natural sandflat and relic reef we sampled based on geomorphological similarities with our experimental reefs constructed on isolated mudflats, this was a surprising result for the natural fringing reef. We note that this natural fringing reef bordered a deep channel, was relatively large (20 m in seaward–landward width and 60 m in along shore width) and was connected to a relatively narrow saltmarsh (10 m in seaward–landward width). Therefore, this reef may have functioned more like an isolated reef, highlighting the context-dependency of carbon burial within reefs. Natural-reef data also suggest that the magnitude of CO₂ flux from restored, intertidal reefs on mudflats related to inorg-C burial must attenuate over time from the high values we observed. This would follow from the initial, rapid accretion of constructed reefs as they rose toward a growth ceiling defined by sea level [30], and subsequent slower accretion bounded by sea-level rise. Conversely, for those fringing reefs that were not accreting fast enough to keep pace with sea-level rise, their role in capturing more carbon would



Figure 4. Shellfish reefs facilitate expansion of other blue carbon habitats. (a) Representative oyster reef–saltmarsh interface soon after the reef was created. (b) Seaward expansion of saltmarsh (*S. alterniflora*) since construction, resulting from the accumulation of sediments within and around the oyster reef. (Online version in colour.)

eventually vanish, although those reefs would continue to play a valuable role as a repository of organic carbon, as well as a rampart to protect the carbon in landward marshes [32].

Although organic:inorganic carbon burial within reefs differs across landscapes, the net effect of habitat destruction for all reefs (whether they functioned as sources of sinks before disturbance) is probably CO₂ release over climate-relevant time scales since excavated organic material may be largely remineralized, while shell may experience continued preservation through reburial. Reburial is particularly likely for the unarticulated shells of disturbed reefs that are no longer defined by the vertical structure of living reefs that rise above the surrounding seafloor/sediments. As with vegetated blue carbon habitats, loss of shellfish reefs could result in the release of formerly dormant organic carbon pools back into the biosphere. Indeed, approximately 20% of current annual anthropogenic CO₂ release is due to habitat modification and destruction [28]. In the broader context of global carbon emissions (7.2–10 billion Mg C yr^{−1}) [4], the anthropogenic disturbance of shellfish habitat has contributed a comparatively small yet significant amount (approx. 400 million Mg C from approx. 1700 to present). This estimate presumes, conservatively, the loss of only the top 1 m of shellfish habitat, although in some regions such as Chesapeake Bay, several metres of reef material were excavated [13]. However, existing or currently proposed legal protection preventing further disturbance of shellfish reefs

is extremely limited and typically localized (e.g. no harvest shellfish sanctuaries) relative to the protections provided to vegetated blue carbon habitats. The potential economic benefits of carbon storage in undisturbed shellfish reefs could be included with other ecosystem services in cost–benefit analyses conducted as part of coastal resource management programmes [10].

While there is mounting interest in the role of coastal and oceanic environments in mitigating anthropogenic climate change by inducing long-term (i.e. millennial) burial of carbon, it is crucial to recognize that global CO₂ emissions challenge ecosystem integrity in every environment on Earth and the carbon burial services of blue carbon habitats are likely to evolve as climate changes. Marine communities are already responding to anthropogenic temperature increases (approx. 0.7 °C globally over the last century) via altered primary production or trophic-transfer rates, changes in phenology and poleward distribution shifts [33]. As oceans absorb atmospheric CO₂, carbonic acid formation lowers marine pH and may impact the fitness of calcifying organisms [20,34]. With increasing urgency, data are also needed to explore how climate-change syndromes (e.g. sea-level rise, elevated heterotrophic metabolism in response to temperature rise, saltwater intrusion, increased storms/sedimentation, acidification) will impact the ability of remaining shellfish reefs to mitigate the rate and consequences of anthropogenic CO₂ increases.

Our data represent a first effort to constrain the climate-related services shellfish reefs may provide via carbon burial, and support global efforts to document missing CO₂ sources and sinks. As more reefs are sampled across gradients in depth, salinity, latitude, productivity, shellfish species, hydrodynamic regime, reef-associated community composition (predation and bioerosion intensity) and reef size, a more complete understanding of shellfish reef carbon dynamics should emerge. Additionally, future work

should evaluate: (i) carbon metabolism beneath the TAZ of shellfish reefs; (ii) how much carbon being deposited within shellfish reefs is already recalcitrant; and (iii) the long-term, climate-related effects of decreasing total dissolved inorganic carbon concentrations via shell burial [35]. While researchers pursue these questions, our data reveal that natural and restored oyster reefs have already demonstrated the potential to bury organic carbon at rates similar to mangrove, salt-marsh and seagrass habitats. For the natural reefs we sampled, and the restored reefs on exposed sandflats, this benefit is offset by the simultaneous burial of inorganic carbon that results in the net venting of CO₂ as these reefs grow. Regardless of how reefs function as carbon sources and sinks, however, disturbance of all these reefs probably results in increased atmospheric CO₂. Thus, carbon sequestration and CO₂ release should be considered in concert with a host of other potential ecosystem services to properly evaluate the incentives for shellfish reef conservation.

Data accessibility. All raw data and calculations available at Dryad Digital Repository (<http://dx.doi.org/10.5061/dryad.7nd95>).

Authors' contributions. F.J.F., A.B.R., J.H.G. and M.F.P. conceived the experiments, while R.K.G., N.L.L., C.H.P. and J.T.R. provided design support. F.J.F., A.B.R., J.H.G. and J.T.R. performed the field experiments. F.J.F., A.B.R., R.K.G., M.F.P., and J.T.R. analysed the data and created the figures. F.J.F. drafted the manuscript and the other authors provided editorial advice.

Competing interests. We declare no competing interests.

Funding. This research was supported by funding from the North Carolina Sea Grant (12-HCE-20), a University of North Carolina Research Council Grant, and the National Science Foundation (OCE-1155628; OCE-1635950).

Acknowledgements. M. Alperin, B. Silliman and two anonymous reviewers provided valuable discussions and critiques regarding this research. A. Tyler, E. Theuerkauf, P. Rodriguez, K. Tran, M. Poletti and A. Atencio assisted with shellfish-reef coring and sample analyses.

References

- Duarte C, Middelburg J, Caraco N. 2005 Major role of marine vegetation on the oceanic carbon cycle. *Biogeosciences* **2**, 1–8. (doi:10.5194/bg-2-1-2005)
- Fourqurean JW *et al.* 2012 Seagrass ecosystems as a globally significant carbon stock. *Nat. Geosci.* **5**, 505–509. (doi:10.1038/ngeo1477)
- Donato DC, Kauffman JB, Murdiyarso D, Kurnianto S, Stidham M, Kanninen M. 2011 Mangroves among the most carbon-rich forests in the tropics. *Nat. Geosci.* **4**, 293–297. (doi:10.1038/ngeo1123)
- Nellemann C, Corcoran E, Duarte CM, Valdés L, De Young C, Fonseca L, Grimsditch G. 2009 *Blue carbon*. Nairobi, Kenya: United Nations Environment Programme.
- Waycott M *et al.* 2009 Accelerating loss of seagrasses across the globe threatens coastal ecosystems. *Proc. Natl Acad. Sci. USA* **106**, 12 377–12 381. (doi:10.1073/pnas.0905620106)
- Council on Climate Preparedness and Resilience. 2014 *Priority agenda: enhancing the climate resilience of America's natural resources*. Washington, DC: Executive Office of the President of the United States.
- Intergovernmental Panel on Climate Change (IPCC). 2013 *Adoption and acceptance of the '2013 supplement to the 2006 guidelines: wetlands'*. Geneva, Switzerland: IPCC.
- Beck MW *et al.* 2011 Oyster reefs at risk and recommendations for conservation, restoration, and management. *Bioscience* **61**, 107–116. (doi:10.1525/bio.2011.61.2.5)
- zu Ermgassen PSE *et al.* 2012 Historical ecology with real numbers: past and present extent and biomass of an imperilled estuarine habitat. *Proc. R. Soc. B* **279**, 3393–3400. (doi:10.1098/rspb.2012.0313)
- Grabowski JH, Brumbaugh RD, Conrad RF, Keeler AG, Opaluch JJ, Peterson CH, Piehler MF, Powers SP, Smyth AR. 2012 Economic valuation of ecosystem services provided by oyster reefs. *Bioscience* **62**, 900–909. (doi:10.1525/bio.2012.62.10.10)
- Dame RF, Spurrier JD, Zingmark RG. 1992 In situ metabolism of an oyster reef. *J. Exp. Mar. Biol. Ecol.* **164**, 147–159.
- Newell R, Langdon CJ. 1986 Digestion and absorption of refractory carbon from the plant *Spartina alterniflora* by the oyster *Crassostrea virginica*. *Mar. Ecol. Prog. Ser.* **34**, 105–115. (doi:10.3354/meps034105)
- DeAlteris JT. 1988 The geomorphic development of Wreck Shoal, a subtidal oyster reef of the James River, Virginia. *Estuaries* **11**, 240–249. (doi:10.2307/1352010)
- Cebrian J. 1999 Patterns in the fate of production in plant communities. *Am. Nat.* **154**, 449–468. (doi:10.1086/303244)
- Coen LD, Brumbaugh RD, Bushek D, Grizzle R, Luckenbach MW, Posey MH, Powers SP, Tolley SG. 2007 Ecosystem services related to oyster restoration. *Mar. Ecol. Prog. Ser.* **341**, 303–307. (doi:10.3354/meps341303)
- Ware JR, Smith SV, Reaka-Kudla ML. 1992 Coral reefs: sources or sinks of atmospheric CO₂? *Coral Reefs* **11**, 127–130.
- Martin S, Clavier J, Chauvaud L, Thouzeau G. 2007 Community metabolism in temperate maerl beds. I. Carbon and carbonate fluxes. *Mar. Ecol. Prog. Ser.* **335**, 19–29.

18. Martin S, Thouzeau G, Richard M, Chauvaud L, Jean F, Clavier J. 2007 Benthic community respiration in areas impacted by the invasive mollusk *Crepidula fornicata*. *Mar. Ecol. Prog. Ser.* **347**, 51–60. (doi:10.3354/meps07000)
19. Matsumoto K, Sarmiento JL, Brzezinski M. 2002 Silicic acid leakage from the Southern Ocean: a possible explanation for glacial atmospheric $p\text{CO}_2$. *Global Biogeochem. Cycles* **16**, 5-1–5-23. (doi:10.1029/2001GB001442)
20. Lerman A, MacKenzie FT. 2005 CO_2 air-sea exchange due to calcium carbonate and organic matter storage, and its implications for the global carbon cycle. *Aquat. Geochem.* **11**, 345–390. (doi:10.1007/s10498-005-8620-x)
21. Waldbusser GG, Powell EN, Mann R. 2013 Ecosystem effects of shell aggregations and cycling in coastal waters: an example of Chesapeake Bay oyster reefs. *Ecology* **94**, 895–903. (doi:10.1890/12-1179.1)
22. Bahr LM, Lanier WP. 1981 *The ecology of intertidal oyster reefs of the South Atlantic coast: a community profile*. Washington, DC: USFWS.
23. Grabowski JH, Hughes AR, Kimbro DL, Dolan MA. 2005 How habitat setting influences restored oyster reef communities. *Ecology* **86**, 1926–1935. (doi:10.1890/04-0690)
24. Reimer PJ *et al.* 2013 IntCal13 and Marine13 radiocarbon age calibration curves 0–50,000 years cal BP. *Radiocarbon* **55**, 1869–1887. (doi:10.2458/azu_js_rc.55.16947)
25. Galtsoff PS. 1967 The American Oyster *Crassostrea virginica* Gmelin. *Fish. Bull.* **64**, 1–480.
26. Dürr HH, Laruelle GG, van Kempen CM, Slomp CP, Meybeck M, Middelkoop H. 2011 Worldwide typology of nearshore coastal systems: defining the estuarine filter of river inputs to the oceans. *Estuaries Coast.* **34**, 441–458. (doi:10.1007/s12237-011-9381-y)
27. Fodrie FJ *et al.* 2014 Classic paradigms in a novel environment: inserting food-web and productivity lessons from rocky shores and saltmarshes in to biogenic reef restoration. *J. Appl. Ecol.* **51**, 1314–1325.
28. Mcleod E, Chmura GL, Bouillon S, Salm R, Björk M, Duarte CM, Lovelock CE, Schlesinger WH, Silliman BR. 2011 A blueprint for blue carbon: toward an improved understanding of the role of vegetated coastal habitats in sequestering CO_2 . *Front. Ecol. Environ.* **9**, 552–560. (doi:10.1890/110004)
29. Davis JL, Currin CA, O'Brien C, Raffenburg C, Davis A. 2015 Living shorelines: coastal resilience with a blue carbon benefit. *PLoS ONE* **10**, e0142595 (1–18).
30. Rodriguez AB *et al.* 2014 Oyster reefs can outpace sea-level rise. *Nat. Clim. Change* **4**, 493–497. (doi:10.1038/nclimate2216)
31. Meyer DL, Townsend EC, Thayer GW. 1997 Stabilization and erosion control value of oyster cultch for intertidal marsh. *Restor. Ecol.* **5**, 93–99. (doi:10.1046/j.1526-100X.1997.09710.x)
32. Ridge JT, Rodriguez AB, Fodrie FJ. 2017 Salt marsh and fringing oyster reef transgression in a shallow temperate estuary: implications for restoration, conservation and blue carbon. *Estuaries Coast.* **40**, 1013–1027. (doi:10.1007/s12237-016-0196-8)
33. McCarty JP. 2001 Ecological consequences of recent climate change. *Conserv. Biol.* **15**, 320–331. (doi:10.1046/j.1523-1739.2001.015002320.x)
34. Orr JC *et al.* 2005 Anthropogenic ocean acidification over the twenty-first century and its impact on calcifying organisms. *Nature* **437**, 681–686. (doi:10.1038/nature04095)
35. Hansell DA. 2013 Recalcitrant dissolved organic carbon fractions. *Annu. Rev. Mar. Sci.* **5**, 421–445. (doi:10.1146/annurev-marine-120710-100757)